Electronic Supplementary Information for the paper:

Prosperity is associated with instability in dynamical networks

Matteo Cavaliere, Sean Sedwards, Corina E. Tarnita, Martin A. Nowak, Attila Csikász-Nagy

Table of Contents

S1 Supporting Methods

S1.1 Details on figure captions

Here we present more detailed descriptions of the figures of the main text.

Fig. 2 shows the typical results of a simulation with a network of $N = 100$ nodes, $b/c = 3$, $p = 0.6$, $q = 0.85$, $u = 0.0001$, $\delta = 0.01$ when the initial random network contains only cooperators. The network visualizations shown in Fig. 2 (d)-(h), Fig. 5 and Fig. S16 are generated using a force directed layout algorithm which treats the links as springs and tries to minimize the forces in the network. Nodes repel each other but are constrained by links which have a 'natural' length (applying no force) and which apply repulsive and attractive forces when compressed or stretched, respectively. The result is an intuitive interpretation which associates high connectivity with high visual compactness.

Fig. 3 shows the average behaviour of transitions from 100 to 0 cooperators (A) and transitions from 0 to 100 cooperators (B) for various embedding parameters p and q. The data for each combination of embedding parameters is generated from two simulation runs of 10^8 steps, starting from a random network of either all cooperators or all defectors. Other parameters are: 100 nodes, $b/c = 3$, $u = 0.0001$, $\delta = 0.01$. Each panel of figures contains individual plots of transitions, in terms of numbers of cooperators (blue) and size of largest network component (black), giving their averages with solid lines and the 10% (lower bound) and 90% (upper bound) quantiles of the observed transitions. Extended versions of these plots are presented below as Fig. S8 and S9, where we show the same plots and the number of observed transitions for the whole range of p,q values.

Fig. 4 presents various statistics concerning two simulation runs of 10^8 simulation steps, excluding the first 10^6: one obtained with an initial network of only cooperators, one with an initial network of only defectors. Starting from these initial networks and ignoring the initial data serves to eliminate the possible influence of initial conditions on the obtained averages. We investigated various benefit to cost ratios of the game by keeping $b = 10$ and setting c accordingly. Fig. 4 shows the *long term* cooperation, largest component and connectivity. We also plot the number of observed transitions during the simulation run and the long term prosperity.

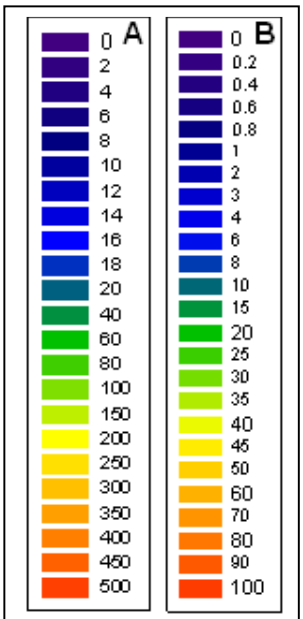

Fig. S1: Tri-linear scale for (A) number of transition and (B) connectivity and prosperity plots

Each panel in the figure was created from a grid of points, corresponding to various combinations of embedding parameters. These are described as the probability of connecting a newcomer to its role model ($p \in \{0, 0.1, \ldots, 1\}$) and the probability of connecting the newcomer to its role model's neighbours ($q \in \{0, 0.2, 0.4, 0.6, 0.7, 0.75, 0.8, 0.85, 0.9, 0.95, 1\}$). Intermediate points were interpolated by the plotting software tool *Sigmaplot* (*Systat Software Inc.*). In Fig. 4 the panels are arranged in columns corresponding to different benefit to cost ratios (b/c).Note the tri-linear scale (Fig. S1) used in Fig. 4 to characterize the long term prosperity, connectivity measures and number of transitions, which are all slowly increasing from 0, but sharply rise at larger values as p and q increase.

Fig. 5 Traces were generated by performing pairs of simulation runs of 10^8 steps, with $p = 0.6$ and $q \in \{0, 0.1, \ldots, 0.6, 0.65, \ldots, 0.8, 0.82, \ldots, 1\}$. The resulting statistics

were plotted and joined by smooth splines. The boundaries of the shaded areas were found by performing separate simulation runs with $u = 0$, starting with either all-cooperator or all-defector networks.

Fig. 6 To find 'typical' networks, sufficiently long and many simulation runs were performed to find 'typical' transitions; a typical transition being one that resembles the median transition for a given set of embedding parameters, in terms of numbers of cooperators, connectivity and largest component over time. Between 8 and 16 transitions were generated per q value, with the approximate long term frequencies of the transitions being 3×10^{-8} for $q = 0.3$, 4×10^{-10} for $q = 0.6$, 4×10^{-8} for $q = 0.75$ and 1.8×10^{-6} for $q = 0.9$. Having chosen a suitable transition, networks containing all-cooperators, all-defectors and approximately equal numbers of cooperators and defectors were found before, after and during the transitions, respectively. In each case the networks were chosen to have connectivity and largest component approximately equal to their means for the given numbers of cooperators and embedding parameters.

S2 Supporting text and figures

Here we complement the analysis presented in the main text. We analyze the system under neutral selection, present a detailed proof for an analytical solution valid in the limit of weak selection and show its agreement with the computational model. We also present the robustness analysis of the observed phenomena.

S2.1 System properties under neutral selection

To evaluate the absence of selection on the dynamics of the model we consider the case of *neutral selection* that is obtained by setting $\delta = 0$. In this way the strategies of cooperator and defector are just arbitrary labels and all nodes obtain an equal effective payoff, independent of their connectivity, and thus have the same chance to be selected as a role-model. This leads to a Moran process extended with mutation between two types of nodes (Moran, 1962; Nowak, 2006). Even with neutral selection, we observe transitions between networks of all cooperators and of all defectors, as evidenced by the data shown in the fourth row, first column of Fig. 4. However, the absence of selection breaks the correlation between network structure and the numbers of cooperators. This independence is apparent in the upper panel of Fig. S2, where the transitions in numbers of cooperators have no visible effect on the plotted network parameters, distinct from what can be observed in Fig. 2. On the other hand, when selection is absent the embedding parameters still control the topology of the networks produced during the process (as can be observed in the lower part of Fig. S2). This is of particular interest because, as shown in the mathematical analysis (Section S2.2), in the limit of weak selection, the minimum b/c favouring cooperation is independent of the parameter p.

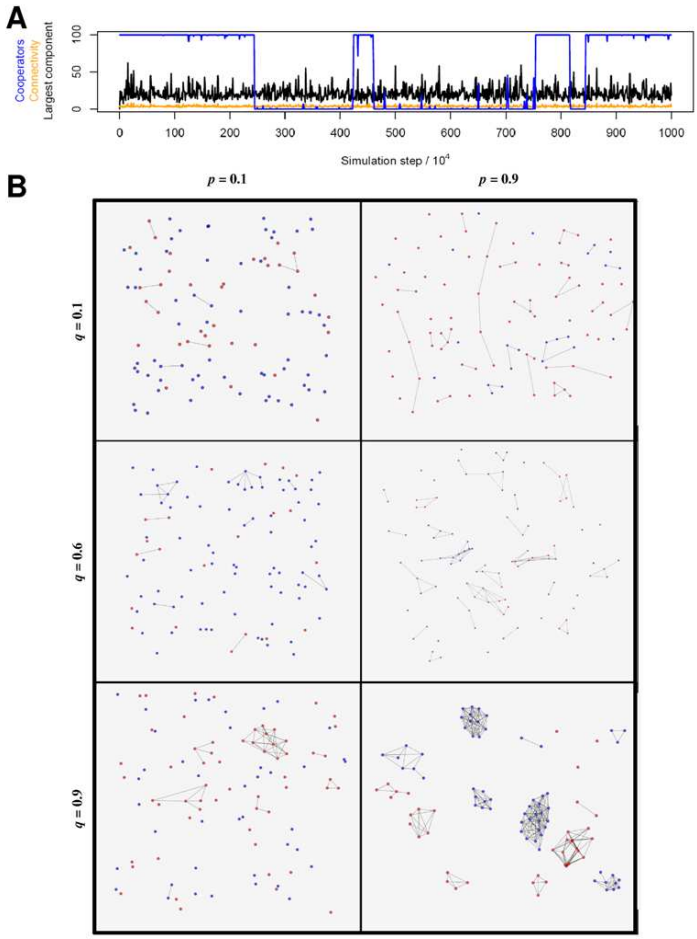

Fig. S2: Typical simulation run and network topologies with neutral selection. A Typical simulation run of 10^7 steps for 100 nodes with neutral selection. Parameters $p = 0.6$, $q = 0.85$, $u = 0.001$ are the same as those used in Fig. 2. **B** Typical networks produced under neutral selection during a transition (p and q parameters are noted on the figure, u is as for A). As can be observed, during the transitions cooperators and defectors (blue and red nodes, respectively) usually exist in separate components. The connectivity and the size of the largest component of the network evidently depend on both embedding parameters p and q (as is the case when selection is included - see corresponding panels in Fig. 4). Network visualisations in this figure were produced by CoSBiLab Graph (Valentini and Jordán, 2010), available from http://www.cosbi.eu/index.php/prototypes/graph.

One can construct a stochastic matrix with the transition probabilities of the neutral process. For $u > 0$, the steady state distribution of the Markov chain can be found, thus expressing the long term average probability of all the possible numbers of cooperators. The results of this calculation for 100 nodes and a range of values of u are shown in Fig. S3.

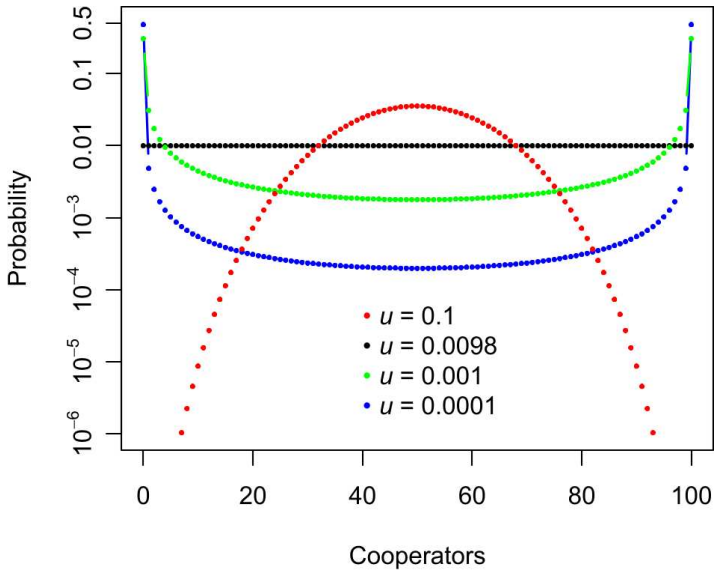

Fig. S3. Chart showing the long term probability of numbers of cooperators for a network of 100 nodes under neutral selection. The network does not play a part in these distributions, which are therefore independent of embedding parameters *p* and *q*.

Fig. S3 shows that for $u << 0.0098$ (green and blue traces) the distribution contains two peaks of high probability at 0 and 100 cooperators, with low probability in between. This intuitively correlates with the dynamics of the simulation traces of numbers of cooperators, which use various mutation rates in the range $0.0002 \geq u \geq 0.00005$. At mutation rates closer to $u \approx 0.0098$ the results in Fig. S3 predict that the system will not strongly favour any particular number of cooperators, while the system will favour a range of values centred on 50 cooperators when $u >> 0.0098$. Simulations (not shown) follow these expectations.

S2.2 Robustness analysis

In this section we show that the phenomena described in the paper are robust: The recurrent transitions (presented in Fig. 2 and Fig. 3) are observed for a wide range of initial parameters, and initial conditions. We also show that the trade-off between prosperity and stability (presented in Fig. 5) is also observed for a wide range of the parameters. Moreover the phenomena are present also when newcomers are drawn from the existing population and keep some of their previous connections (we can say that they have "memory").

S2.2.1 Parameter robustness of transitions

To demonstrate the robustness of the phenomena described in Fig. 2, we present the results of typical simulation runs using parameters which bracket (from half to double) those used to produce Fig. 2. Precisely, we show results for networks with 50 and 200 nodes, with mutation rates $u = 0.0002$ and $u = 0.00005$ and with selection strengths $\delta = 0.02$ and $\delta = 0.005$. In all these cases the results are qualitatively similar to those of Fig. 2. Furthermore, we show that using the same parameters, but starting from an initial network containing all defectors, produces qualitatively similar results to those presented in Fig. 2. For completeness, we also show that the phenomena described in Fig. 2 are not dependent on the method of updating (birth-death or death-birth).

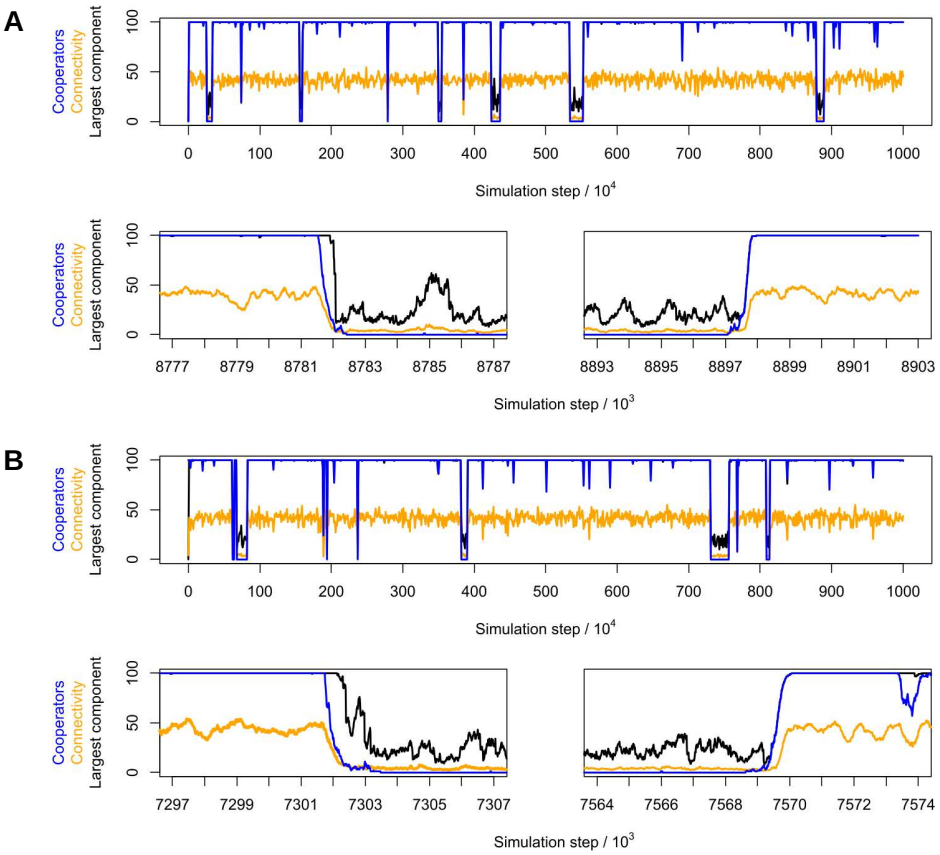

Fig. S4: Typical simulation runs with (A) an initial network of defectors and (B) with Death-Birth updating. Other parameter values are the same as those used in Fig. 2: 100 nodes, $b/c = 3$, $p = 0.6$, $q = 0.85$, $u = 0.0001$ and $\delta = 0.01$. (A) After an initial transition from 100 defectors to 100 cooperators, the traces take on the appearance of those of Fig. 2. (B) The traces produced using Death-Birth updating appear no different to those of A and Fig. 2A, produced by Birth-Death updating. We conclude that the phenomena described in Fig. 2 are neither dependent on the numbers of cooperators present in the initial network, nor by the method of updating.

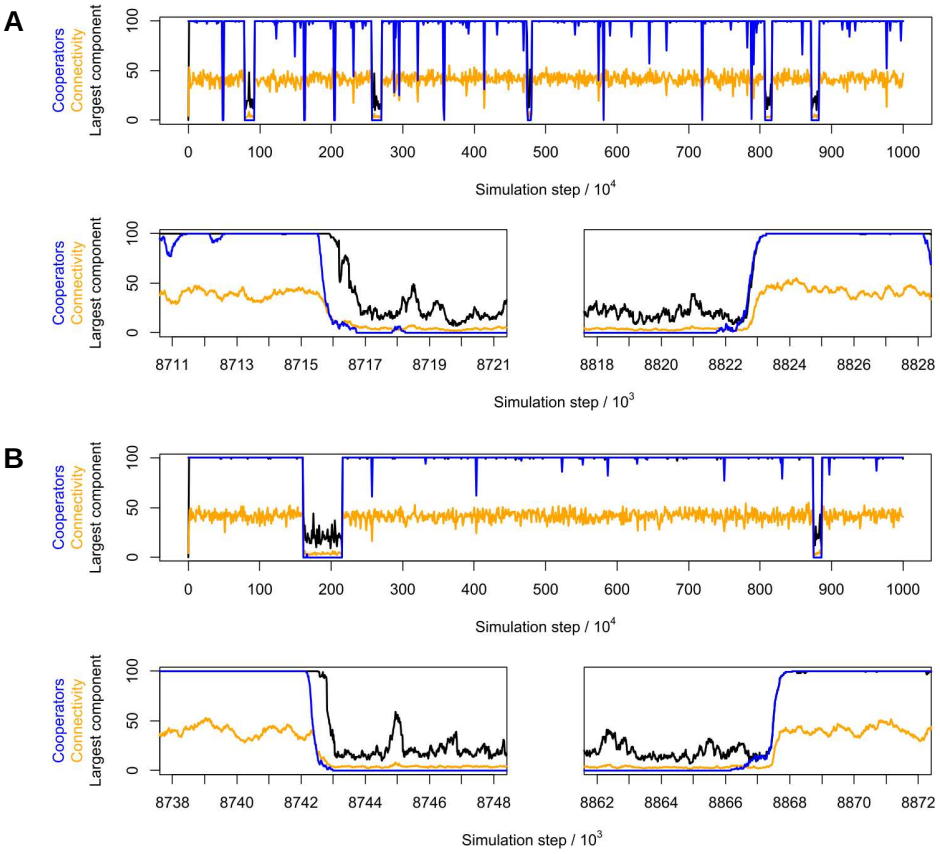

Fig. S5: Typical simulation runs with mutation rate (A) u = 0.0002 and (B) u = 0.00005. Other parameters are the same as those used in Fig. 2. (A) With higher mutation rate, there appears to be more frequent transitions and a greater tendency to move away from the value of 100 cooperators, in comparison to Fig. 2. This might be expected as a consequence of the relation between the dynamics of the model and the mutation rate with neutral selection (Fig. S3). However, qualitatively, the phenomena are the same as presented in Fig. 2. (B) With a lower mutation rate, there are no outstanding features that distinguish the traces from those shown in Fig. 2. Overall, we conclude that the phenomena presented in Fig. 2 are observed for a wide range of mutation rates.

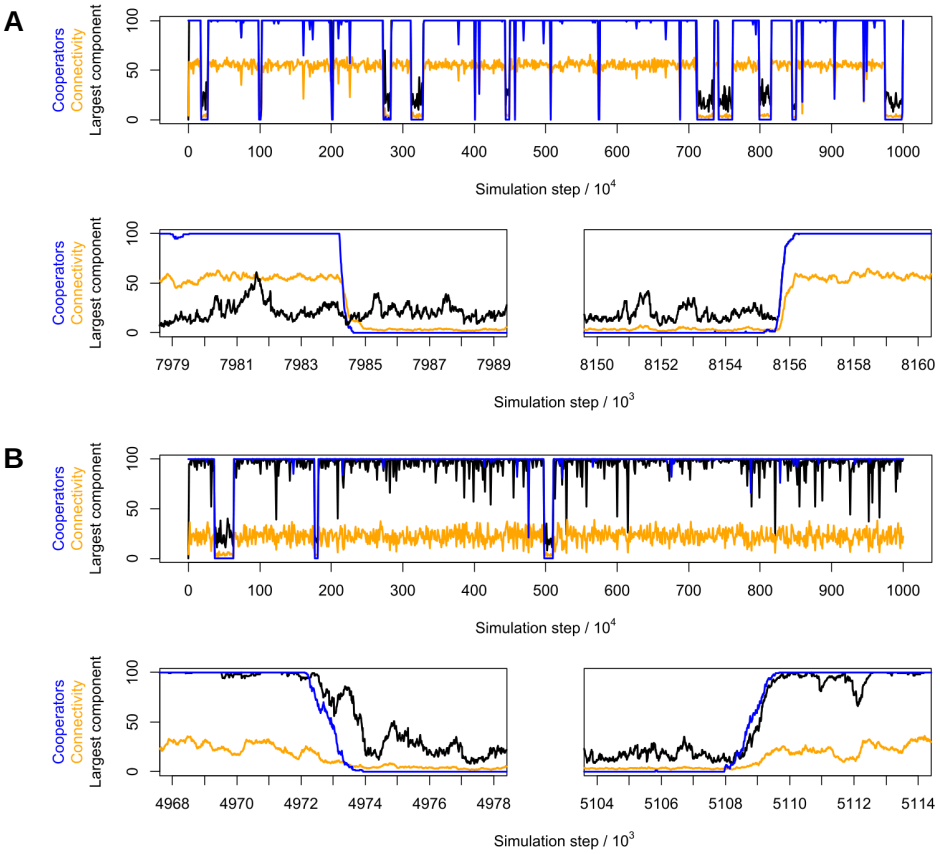

Fig. S6: Typical simulation runs with selection strength (A) δ = 0.02 and (B) δ = 0.005. Other parameters are the same as those used in Fig. 2. (A) With stronger selection there appears to be a higher frequency of transitions and a marginally higher average connectivity. The transitions appear to be faster than the ones in Fig. 2, but qualitatively the phenomena are the same. (B) With weaker selection, the inherent stochasticity is more apparent in the largest component trace, the average connectivity is lower and the transitions are slower, but the phenomena are still similar. Overall, we conclude that the phenomena described in Fig. 2 are observed for a wide range of selection strengths.

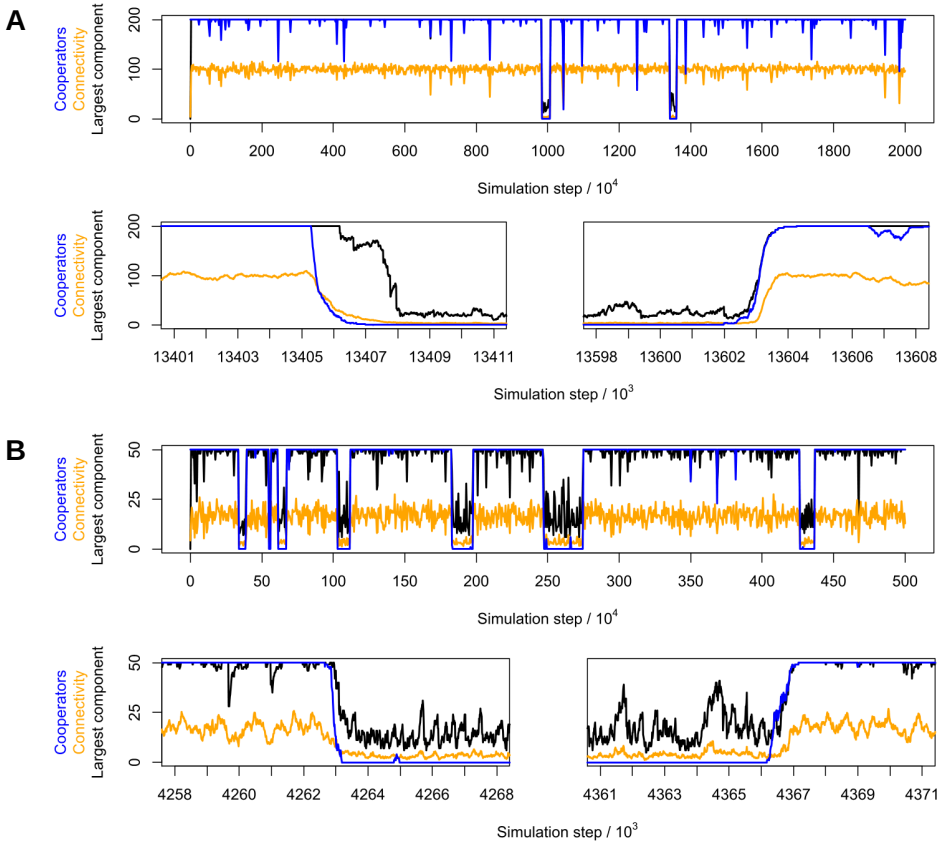

Fig. S7: Typical simulation runs with (A) 200 nodes and (B) 50 nodes. Other parameters are the same as those used in Fig. 2. (A) With a larger network, transitions appear to be slower than the ones shown in Fig. 2, network fragmentation appears to take longer and there appears to be less stochasticity. Other than these differences, which are consistent with the increased numbers of nodes, the phenomena are qualitatively similar to those shown in Fig. 2. (B) With a smaller network, transitions are faster, network fragmentation is more rapid and stochasticity is more evident in the network measures, in relation to the same features of Fig. 2 (which is expected for a network with reduced number of nodes). We conclude that the phenomena described in Fig. 2 are observed for a wide range of network sizes.

S2.2.2 Robustness of transition for embedding parameter changes

We show that the phenomena shown in Fig. 2 are observed for a wide range of embedding parameters p and q. On the following figures we extend Fig. 3 and plot average transitions from the all-cooperators to all-defectors states (Fig. S8), and the reverse (Fig. S9) for the whole p-q parameter plane. These plots show that network fragmentation occurs with a delay after the spreading of defectors, while network formation happens synchronously with the spreading of cooperators. We also note that the delay between the spreading of defectors and the network fragmentation is an increasing function of the embedding parameters, while the time for the network to rebuild is a decreasing function of those parameters.

We can conclude that the correlation between network fragmentation (Fig. S8) and formation (Fig. S9) and the spreading of defectors or cooperators is present for a wide range of embedding parameters. In fact, this correlation was observed wherever we recorded transitions, except at very low p or q values where the evolution of the

network appears to be much less dependent on the evolutionary dynamics of cooperators and defectors. Moreover, there is a large p, q region where no all-defectors to all-cooperators transitions are observed in 10^8 steps.

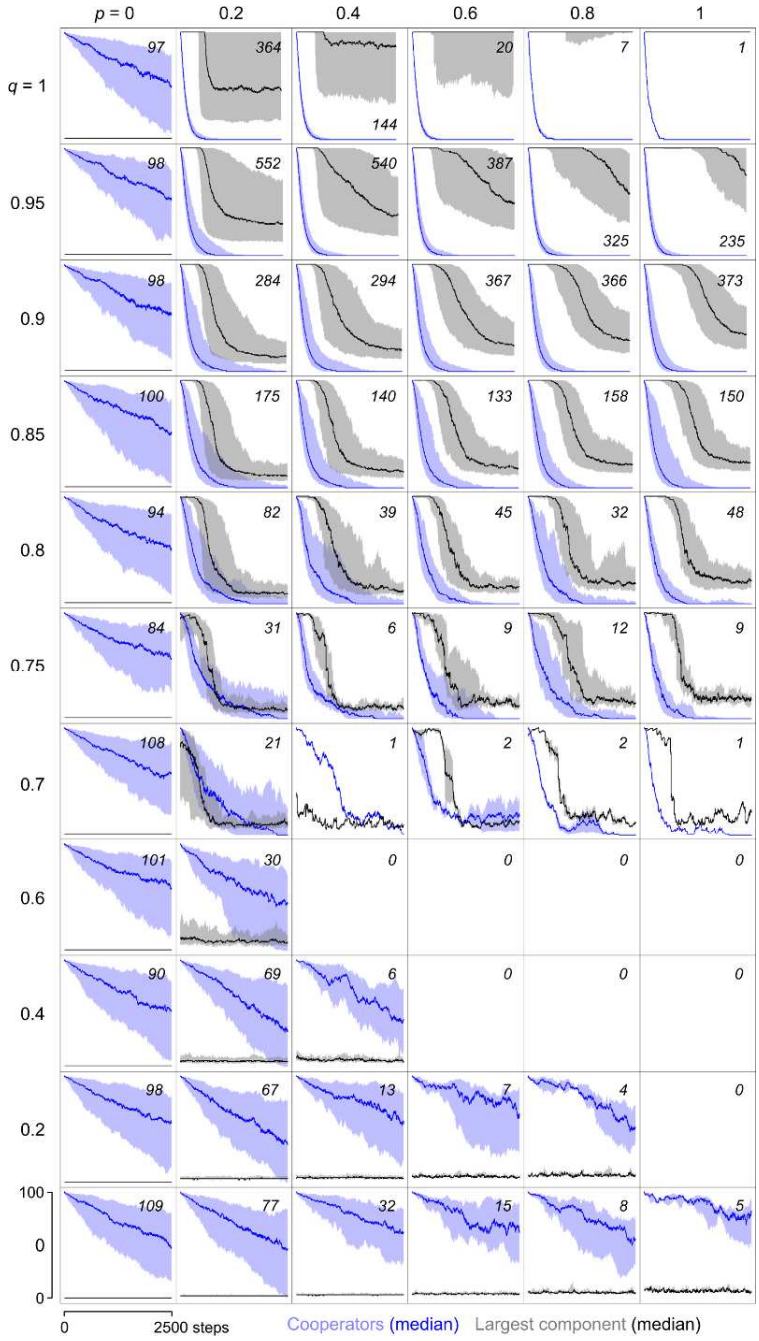

Fig. S8: Statistics of transitions from all cooperators to all defectors at various embedding parameters. Extended version of Fig. 3A of the main text. On each panel we plot the median (dark lines) of amount of cooperators and largest component, calculated considering all the transitions observed in two runs of 10^8 steps, using parameters N = 100, b/c = 3, u = 0.0001. The shaded regions represent the 10% (lower bound) and 90% (upper bound) quantiles for the corresponding measures. The numbers of observed transitions are given in the corner of each panel. Panels which

record zero transitions should not be taken to imply that transitions never occur, but that they are less frequent than 1 in 2×10^8 steps.

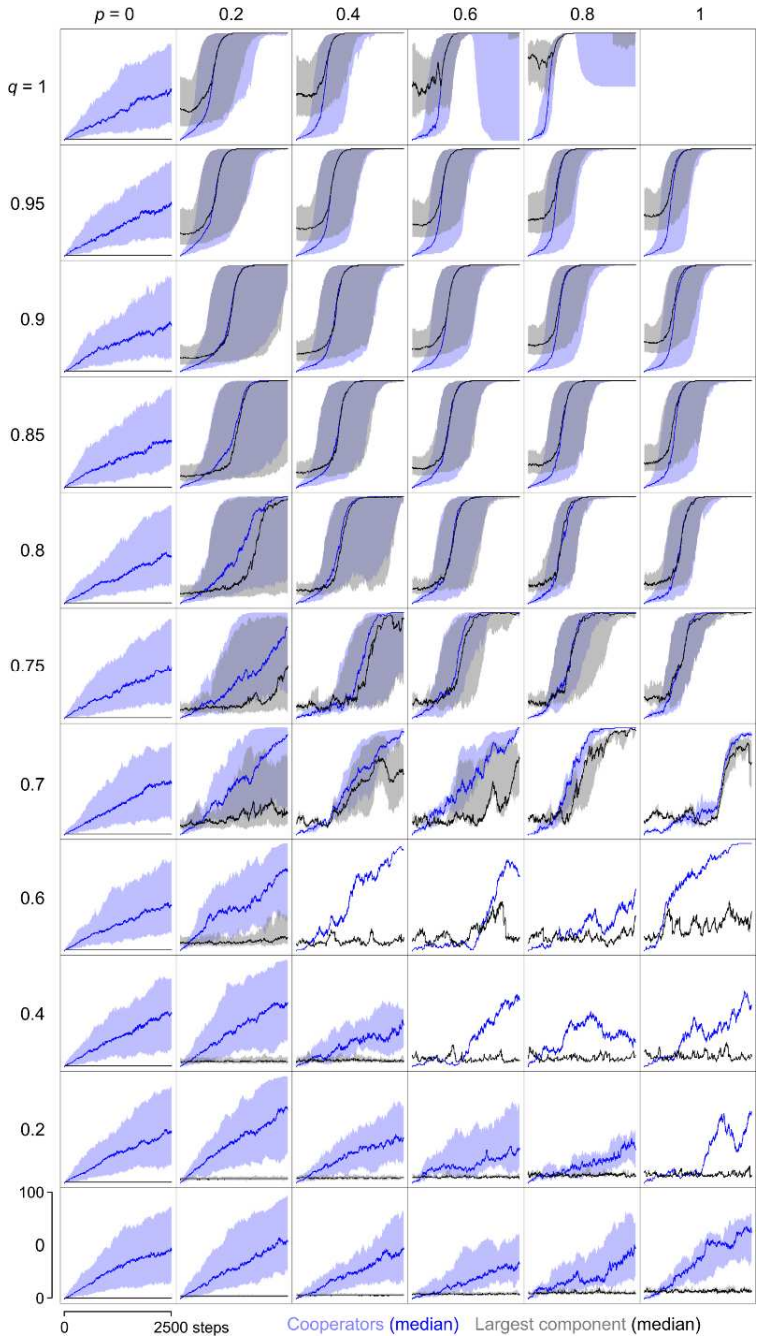

Fig. S9: Statistics of transitions from all-defectors to all-cooperators at various embedding parameters. Extended version of Fig. 3B of the main text. On each panel we plot the median (dark lines) of amount of cooperators and largest component, calculated considering all the transitions observed in two runs of 10^8 steps, using parameters $N = 100$, $b/c = 3$, $u = 0.0001$. The shaded regions represent the 10% (lower bound) and 90% (upper bound) quantiles for the corresponding measures. The numbers of observed transitions (not shown) are equal (±1) to the numbers reported on Fig. S8.

S2.2.3 Robustness of the trade-off between prosperity and stability

We investigated how large changes in the mutation rate and selection strength perturb the trade-off between prosperity and stability observed (Fig. 5) when newcomers connect with high chance to the neighbours of the selected role-model (high q). We show (Fig. S10) that an increase of 10 or even 100 times of the considered mutation rate does not affect the phenomena, as well as a decrease of the selection strength up to 10 times the one used in Fig. 5

S2.2.4 Robustness for the introduction of memory

The model analyzed can be easily enriched with more parameters. One extension of possible interest is presented here. In this case, newcomers are drawn from the existing population and can keep some of their previous connections (we call this "memory"). In this case, at each step of the evolutionary process, the effective payoff of every node is calculated and one node in the network is selected as the role-model, as described in the main text. Then, a randomly selected node in the network, including the chosen role-model, is selected as the newcomer. Both selections are thus made from N nodes, as in the model without memory. The newcomer is assigned the role-model's strategy with probability 1-u or with probability u it mutates to the alternative strategy, as in the model without memory. The newcomer keeps each of its previous links with probability m (*memory*). A link is established between the role-model and each of its neighbours with probability q. When a link is already present, q is treated as zero. With probability p the newcomer is linked to the role model. In the case that the node selected as role model is also selected as newcomer, p is treated as zero, which corresponds to the model without memory when the role model is deleted.

As expected, increasing the value of the memory, m, generally leads to an increase of the connectivity of the network, such that with relatively small p and q values the networks can have high connectivity. Despite this fact, we can show that for a certain regime of the embedding parameters and for non-trivial values of memory, we observe similar phenomena to those seen with the model without memory. A notable consequence of memory, however, is that fragmentation is generally reduced, since memory tends to keep distant parts of the network connected. Specifically, in Fig. S11, obtained for the same parameter values as used in Fig. 2 but with memory, we show that conflicts between cooperators and defectors lead to the formation and fragmentation of the network even when memory is present (qualitatively as in Fig. 2). On Fig. S12 we report the counterpart of the results shown in Fig. 4 for the model with memory $m = 0.1$, where we observe that the area of high long term prosperity and large number of transitions is shifted to lower q values, but the qualitative picture is very similar. Also, the qualitative trade-off between network stability and prosperity (as the ones presented in Fig. 5) is preserved and shown in Fig. S13. These results show that, even using the same parameter values, the observed qualitative phenomena exist also in the model with memory.

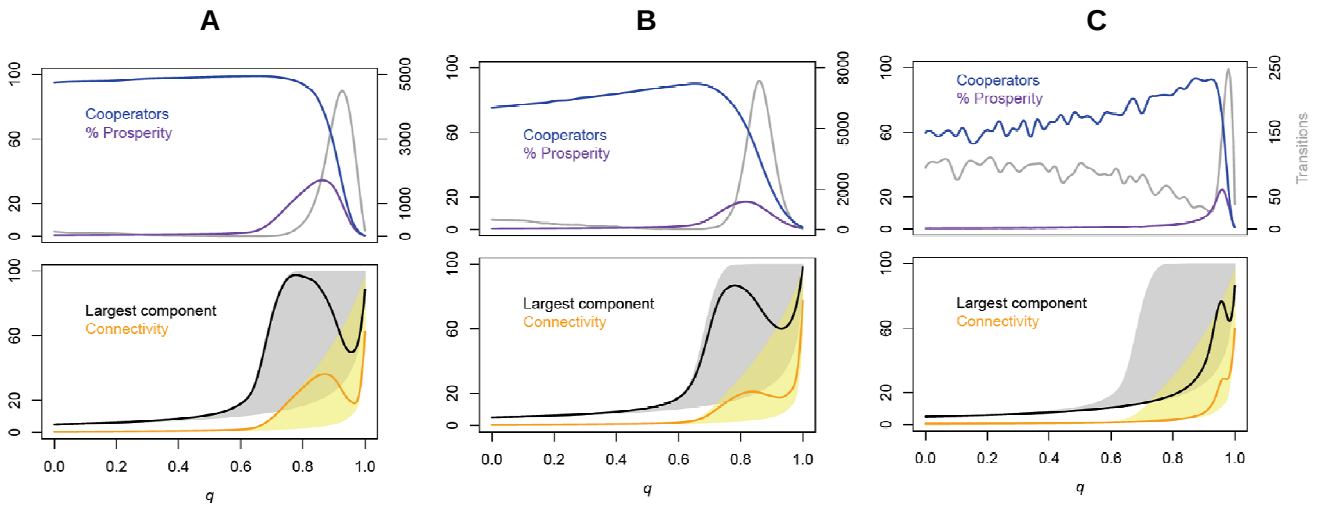

Fig. S10: Trade-off between network stability and prosperity at different mutation and selection rates. Parameter values are the same as those used in Fig. 5 ($b/c = 3$, $N = 100$, $\delta = 0.01$, $u = 0.0001$) except the mutation rate (**A**) $u = 0.001$ (10 times the one considered in Fig. 5), (**B**) $u = 0.01$ (100 times the one considered in Fig. 5) and (**C**) the selection strength $\delta = 0.001$ (1/10 of the one considered in Fig.3).. The qualitative phenomena discussed in Fig. 5 and associated with the increase of parameter q is preserved, albeit the number of transitions increases as the mutation rate is increased (A-B) and decreases (C) as selection becomes weaker (note the differences in the scales denoting the number of transitions). With weaker selection the system starts to approach the neutral selection case (investigated in section S2.1 and S2.2). As selection becomes weaker the regimes of high prosperity and with high number of transition are shifted to higher q values (compared to Fig. 5), but their overlap is still present. With lower selection strength, noise is higher, leading to the more noisy curves. The shaded areas, corresponding to those in Fig. 5, denote the ranges of connectivity (yellow) and largest component (grey) between all-cooperators (upper boundary) and all-defectors (lower boundary).

In contrast to corresponding simulations without memory, shown in Fig. 2, we observe that with $m = 0.1$ the networks less frequently consist of only cooperators (Fig. S11c). However, we observe a similar qualitative picture comparing Figures S12 and S13 with Figures 3 and 4. The quantitative difference on these plots appears as a shift to lower q values approximately equal to m and a reduced drop in the size of the largest component when cooperation declines. However, in certain cases, such quantitative difference with the model without memory can be tuned by choosing appropriate embedding parameter values. For instance, for lower values of the embedding parameters p and q, the transitions lead to much more complete fragmentations of the networks (Fig. S12). In Fig. S14 we illustrate this fact on the simulation traces obtained for a lower embedding parameter p.

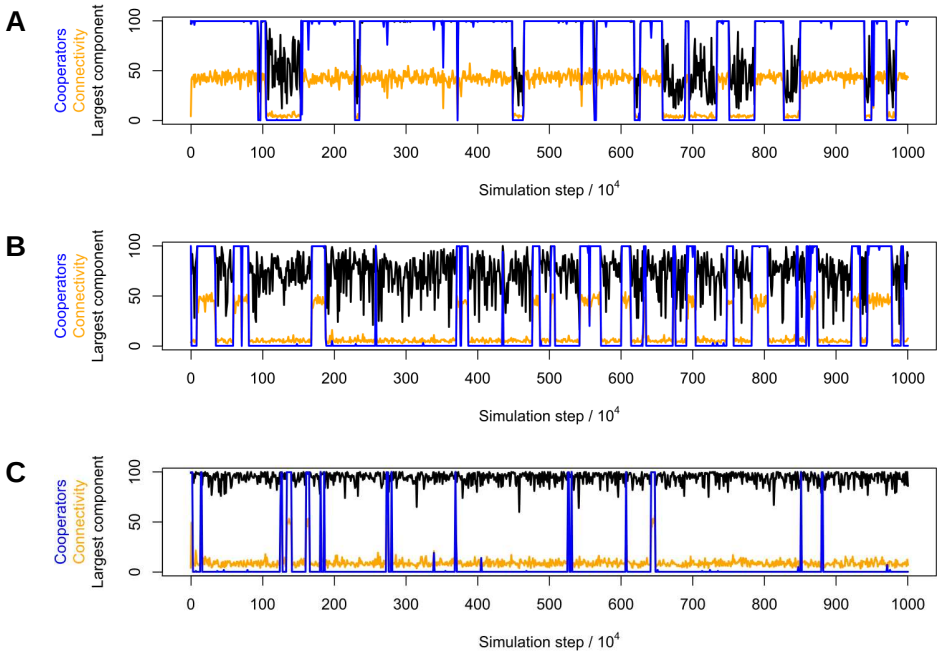

Fig. S11: Typical simulation runs with memory. Parameter values are the same as used in Fig. 2 (b/c = 3, N = 100, δ = 0.01, u = 0.0001) with the addition of memory: (A) m = 0.02, (B) m = 0.05 and (C) m = 0.1. (A) With m = 0.02 (2% of memory) the simulations show frequent transitions and a less fragmented network when the network consists of defectors. (B) at 5% memory the networks consist mostly of defectors, but transitions are still frequent. All nodes are in a single component only when the network consists entirely of cooperators. A network of defectors fragments minimally, but its connectivity is greatly reduced. (C) Defectors are more favoured when memory is equal to 10% but there are still short intervals when highly connected networks of cooperators appear.

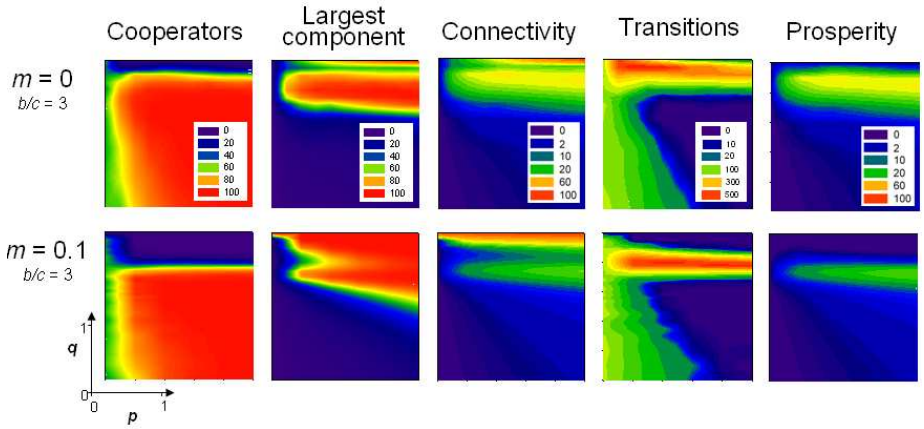

Fig. S12: Results with memory (m = 0.1) and without memory (m = 0) for b/c = 3. Other parameters are N = 100, u = 0.0001, δ = 0.01, as in Fig. 4. Maximum long term prosperity, largest number of transitions and the area of high long term cooperation appear at lower q values with memory, but the qualitative picture remains similar to that without memory.

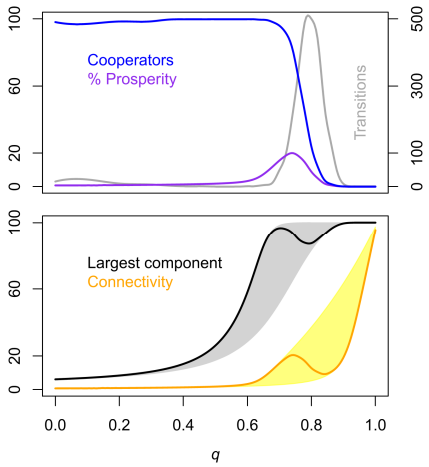

Fig. S13: Trade-off between network stability and prosperity with memory. Parameter values are the same as those used in Fig. 5 (b/c = 3, N = 100, δ = 0.01, u = 0.0001) but with the addition of memory (m = 0.1). The qualitative phenomena associated with increasing q appear to be preserved, albeit shifted by approximately -0.1on the q axis. Notable differences are that memory has the effect of preserving large components when cooperation declines and that maximum prosperity is lower. The shaded areas, corresponding to those in Fig. 5, denote the ranges of connectivity (yellow) and largest component (grey) between all-cooperators (upper boundary) and all-defectors (lower boundary). To generate these traces, pairs of simulations were performed with p = 0.6 and $q \in$ {0, 0.1, ..., 0.4, 0.45, 0.5, 0.52, ..., 1}. The resulting data points were plotted and joined by smooth splines. The boundaries of the shaded areas were found by performing separate simulation runs with u = 0 and starting with either all-cooperator or all-defector networks.

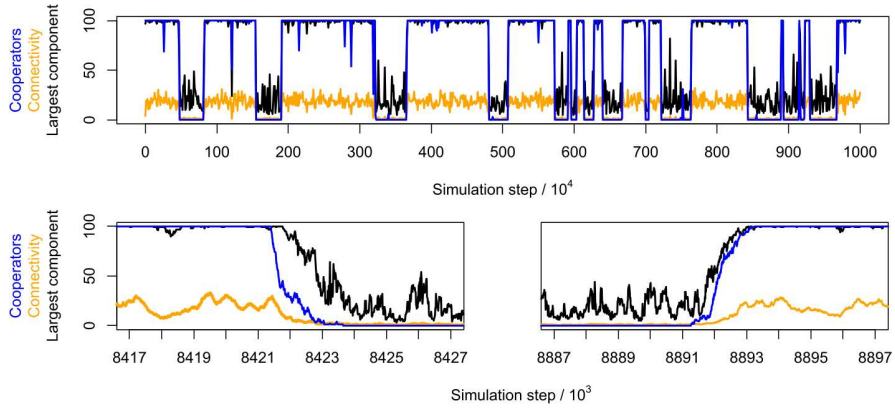

Fig. S14: Typical simulation runs with memory m = 0.1, p = 0.2, q = 0.75 and b/c = 3. Other parameter values are N = 100, u = 0.0001 and δ = 0.01. Networks of cooperators tend to exist in a single connected component, while networks of defectors appear much more fragmented than in the cases shown in Fig. S11.

S2.3 A perspective on Transitions

We have shown in Fig. 4-6 that the embedding parameters influence the observed number of transitions that, in turn, correlates with the maintenance of cooperation and prosperity. A complete investigation of the mechanisms that cause the transitions is left as an interesting open area for future research. Following our simulations, however, we speculate that the transitions are the consequence of the ability of new nodes to connect and remain

connected to cooperators. This is evidenced by Figures S15 and S16. Fig. S15 presents the degree distributions and the average effective payoff associated to cooperator and defector nodes in the networks shown in Fig. 6. As expected, in the networks of only defectors all nodes have uniform average effective payoff, while in the networks of only cooperators, the most connected nodes have the highest average effective payoff. One can observe that a transition from defectors to cooperators is caused by the appearance of a cluster of cooperators with higher average effective payoff than the many small "islands" of defectors. On the other hand, a transition from all cooperators to all defectors is caused by the parasitic exploitation of cooperator nodes: cooperators have many links but these are mostly to defectors that can obtain higher payoff. The ability for defectors to remain connected to cooperators is crucial to their success, since this is the only way they can receive benefits This is illustrated in Fig. S16, which shows an incomplete transition - one of the small, short-lived, drops in cooperation evident in Fig. 2A. When defectors remain isolated from the cooperators in a network, their spreading can be blocked. This can happen, for instance, if the reduction in connectivity between cooperators and defectors leads to a single connecting node which is randomly deleted. When cooperators get isolated from defectors in this way, they can rebuild their network rapidly, as in the case of complete transitions (Fig. 6). Following our simulations, we speculate that such uncoupling of cooperators from defectors could constitute the most important mechanism of stopping defectors spreading.

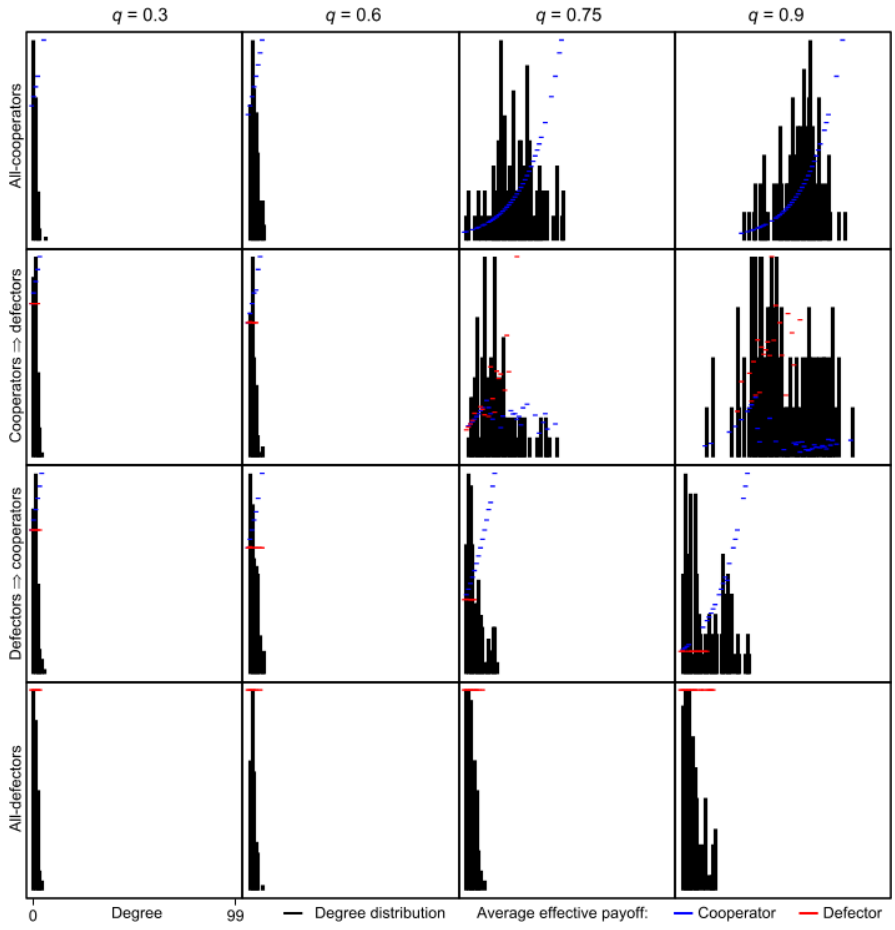

Fig. S15: **Degree distributions and average effective payoff.** Node degree frequency and corresponding average effective payoff for cooperator and defector nodes for the networks presented in Fig. 6. Effective payoff and frequency are scaled with respect to the respective maximum observed.

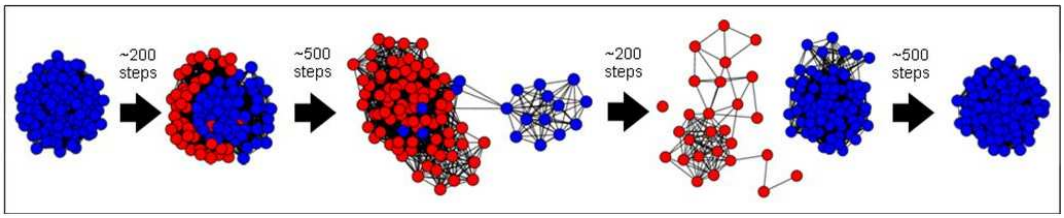

Fig. S16: **Failed invasion of defectors.** A typical incomplete transition with $p = 0.6$, $q = 0.9$: defectors invade most of the network but the populations of cooperators and defectors become separated, allowing cooperators to rebuild their highly connected network.

References

Moran, P.A.P., 1962. The statistical processes of evolutionary theory. Clarendon Press, Oxford.

Nowak, M.A., 2006. Evolutionary Dynamics: Exploring the Equations of Life. Harvard University Press, Cambridge, MA.

Valentini, R., and Jordán, F., 2010. CoSBiLab Graph: The network analysis module of CoSBiLab. Environ Modell Softw 25, 886-888.